Tetrahedron 67 (2011) 6252–6258

Contents lists available at ScienceDirect

Tetrahedron

journal homepage: www.elsevier.com/locate/tet

Phenylethylidene-3,4-dihydro-1*H*-quinoxalin-2-ones: promising building blocks for Cu^{2+} recognition

Efrat Korin [a], Beny Cohen [a,*], Cheng-Chu Zeng [b,*], Yi-Sheng Xu [b], James Y. Becker [a,*]

[a] Department of Chemistry, Ben-Gurion University of the Negev, Beer Sheva 84105, Israel
[b] College of life Science and Bioengineering, Beijing University of Technology, Beijing 100124, China

ARTICLE INFO

Article history:
Received 30 January 2011
Received in revised form 25 May 2011
Accepted 16 June 2011
Available online 22 June 2011

Keywords:
Quinoxalone derivatives
Cu^{2+} recognition
Fluorescence
Chemosensors

ABSTRACT

A series of sulfonamido-substituted phenylethylidene-3,4-dihydro-1*H*-quinoxalin-2-one derivatives in which both of the fluorophore and ionophore are integrated into one structural unit, have been investigated. They all exhibit high selectivity toward Cu^{2+} in ethanol in the presence of other metallic ions (Zn^{2+}, Mg^{2+}, Co^{2+}, Ni^{2+}, Mn^{2+}, Ca^{2+}, and Ag^{+}), as well as fast, stable, and reversible binding, as is evidenced by the observation of a red shift in the UV–vis spectrum, 'ON–OFF' fluorescence response. In addition, titration and MALDI-TOF measurements indicated that a 1:1 (and possibly also 2:1 (organic ligand: Cu^{2+}) complexes were formed, depending on the relative amount of Cu^{2+} added to the solution of the organic ligand. It was also found that the binding constant could be tuned by modifying the nature and position of the substituents attached to the central benzene ring in the quinoxalone derivative. In acetonitrile, unlike in ethanol, these ligands undergo oxidation-decomposition by Cu^{2+} and therefore, no UV–vVis absorption bands could be observed. However, due to color change (from yellow to transparent) they could be useful as dosimeters in this solvent.

1. Introduction

The development of synthetic optical sensors for essential heavy metallic ions continues to attract a considerable research interest due to their important role in living systems and their impact on environmental toxicity.[1,2] Based on the different pathways for ion sequestration, these sensors can be divided into two categories: 'fluorogenic' chelating agents (e.g., 8-hydroxyquinoline[3]) and 'fluoroionophores' with separate fluorophore and ionophore units, in which the fluorophore responses for signal transduction and the ionophore for selective recognition of metal ions.

Among the heavy metallic ions, Cu^{2+} is important because it is the third most abundant (after Fe^{3+} and Zn^{2+}) among essential heavy metals in the human body and it is important in various physiological processes. In addition, Cu^{2+} is a significant environmental pollutant. For these reasons, the past few years have witnessed a number of reports on the design and synthesis of optical or fluorescent sensors for the detection of Cu^{2+} ions.[4–9] Gunnlaugsson et al.[10] designed an azobenzene-based colorimetric chemosensor, which could detect Cu^{2+} under physiological conditions and give rise to a major color change from red to yellow. Molina[11] reported on several colorimetric and fluorescent chemosensors with azine or 2-aza-1,3-diene moieties as putative cation-binding sites, where anthracene or pyrene serves as fluorophores for signal transduction. The latter property is based on photo-induced intramolecular electron-transfer (PET) mechanism or fluorescence quenching caused by the paramagnetic nature of Cu^{2+}.

In parallel studies, diketo acid derivatives have been demonstrated[12–14] to be among the most promising HIV integrase inhibitors, which are able to selectively inhibit a strand transfer reaction of integrase in vitro and in infected cells. The molecular basis of inhibition of this type of compounds is the sequestration of the critical metal cofactor(s) (Mg^{2+} is now generally accepted) in the integrase active site. In this context, the binding of a divalent metal ion (Mg^{2+}) is a prerequisite for the HIV integrase inhibition.

Base on the above mentioned information, recently we have carried out a project to design and synthesize sulfonamido-, caffeoyl- and galloyl-containing diketo acids, and quinoxaline-2-ones, as potential HIV integrase inhibitors[15,16] However, the latter derivatives did not bind Mg^{2+} but showed selective response toward Cu^{2+}. In the present work, we report new results of phenylethylidene-3,4-dihydro-1*H*-quinoxalin-2-ones (involving integrated fluorophore and ionophore units) as promising building blocks for selective recognition of Cu^{2+}. It is noteworthy that this system is unique because other known fluorogenic chelating agents, such as 8-hydroxyquinoline[3] have shown low selectivity toward various divalent metal cations.

* Corresponding authors. Tel.: +972 8 6461197; fax: +972 8 6472943 (J.Y.B.); tel.: +972 8 646 1639; fax: +972 8 6472943 (B.C.); tel.: +86 10 67396211; fax: +86 10 67392001 (C.-C.Z.); e-mail addresses: bcohen@bgu.ac.il (B. Cohen), zengcc@bjut.edu.cn (C.-C. Zeng), becker@bgu.ac.il (J.Y. Becker).

0040-4020/$ – see front matter © 2011 Elsevier Ltd. All rights reserved.
doi:10.1016/j.tet.2011.06.047

2. Results and discussion

The structures of quinoxaline-2-one derivatives **3** and **4** are shown in Scheme 1. These compounds were synthesized in >90% yield according to our previous report.[15] A mixture of **1** or **2** and *o*-phenylenediamine in water was heated to reflux for 2–4 h and the desired **3** or **4** was isolated after cooling, filtering, and washing with ether. The products are yellowish solids and exhibit strong fluorescence under UV–vis excitation at 365 nm.

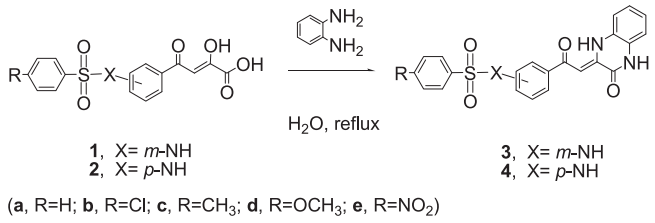

Scheme 1. Synthesis of compounds **3** and **4**.

2.1. UV–vis spectra of 3 and 4 in ethanol

The absorption spectra of **3** and **4** in ethanol solutions were investigated and a typical spectrum of compound **4b** is shown in Fig. 1. In the absence of metallic ions, all these compounds display a shoulder band at 392 nm and two intense absorption bands centered at about 418 and 441 nm in the visible region with extinction coefficients of 3.1×10^4 and 2.8×10^4 $Lmol^{-1}\,cm^{-1}$, respectively. The intense and low-energy absorptions of compounds **3** and **4** in the visible region suggest a $\pi-\pi^*$ transition (K band) taking place in these conjugated systems, which has also been supported by their X-ray structures. For example, in compounds **3a**,[17] **4b**,[15] and **4d**,[18] the two nitrogen atoms in the quinoxalone ring are of sp^2 hybridization, resulting in a planar arrangement of the quinoxalone ring. Moreover, an intramolecular N–H···O hydrogen-bond is present and allows the quinoxalone ring and the 2-oxo-ethylidene unit to be in the same plane.

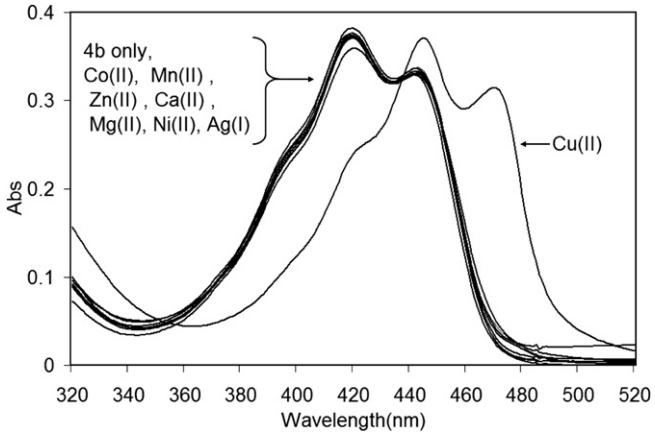

Fig. 1. UV–vis absorption spectra of **4b** in the absence and presence of 100 equiv of metal ions in ethanol; [**4b**]=1.2×10^{-5} mol/L.

2.2. The effect of different metal ions on the UV–vis and fluorescence spectra of 3 and 4 in ethanol

Fig. 1 presents the absorption spectra of **4b** in the presence of 100 equiv of metallic ions in ethanol (large excess of cations have been used in order to prove the specific binding of Cu^{2+} and the lack of binding of other cations). Clearly no significant change in the spectra takes place when more than 100 equiv of Zn^{2+}, Mg^{2+}, Co^{2+}, Ni^{2+}, Mn^{2+}, Ca^{2+}, and Ag^+ were added. However, when $Cu(ClO_4)_2$ was added, each of the three absorption bands at 392, 419, and 442 nm undergoes a red shift by 26–28 nm, with concomitant appearance of three new absorption bands at 421, 445, and 470 nm (it is noteworthy that under these conditions, $Cu(ClO_4)_2$ has no absorption above 320 nm). Moreover, upon addition of EDTA as a strong complexing agent, the original absorption bands (at 392, 419, and 442 nm) of **4b** re-appeared, indicating the existence of a reversible process.

The absorptions and ion binding properties of other derivatives of types **3** and **4** exhibit similar patterns to those of **4b**. Their absorption maxima and wavelength changes in the presence of Cu^{2+} are summarized in Table 1. The red shift observed after the addition of $Cu(ClO_4)_2$ to a solution of the organic ligand can be attributed to deprotonation of one of the secondary amine moieties in the quinoxalone ring. Accordingly, the UV–vis spectrum of free **3b** (2.4×10^{-5} M) in the presence of NaOH (5×10^{-3} M) also exhibits a red shift (although smaller, ~14 nm) compared to the spectrum without the base, emphasizing the effect of deprotonation (see Supplementary data). To confirm that the red shift observed upon addition of NaOH was not due to Na^+ ions, $NaClO_4$ (1.4×10^{-2} M) was added to **3b** (2.4×10^{-5} M) and no change in the spectrum was observed.

Table 1
Change of absorption peaks ($\lambda_{max}\pm0.5$ nm) of compounds **3** and **4** in the presence of Cu^{2+} in EtOH

'Host'	λ^1_{max}	λ^2_{max}	λ^3_{max}	'Host'	λ^1_{max}	λ^2_{max}	λ^3_{max}
3a	395[a] (416)[b]	416 (442)	442 (470)	**4a**	394 (420)	418 (444)	444 (472)
3b	393 (419)	418 (441)	440 (465)	**4b**	392 (421)	419 (445)	442 (470)
3c	394 (418)	418 (440)	439 (466)	**4c**	396 (422)	420 (444)	441 (471)
3d	395 (416)	416 (443)	442 (467)	**4d**	395 (422)	419 (445)	441 (471)
3e	395 (—)	417 (444)	445 (470)	**4e**	395 (421)	418 (445)	444 (472)

[a] Absorption wavelength (λ_{max}) of free compounds (throughout the Table).
[b] Absorption wavelength (λ_{max}) of compounds after addition of Cu^{2+}(in parentheses, throughout the Table).

Additional proof about the origin of the red shift stems from the effect of acid addition to the complex solution, which was investigated by both UV–vis and EPR measurements. In each technique the addition of $HClO_4$ to a solution of **3b** containing Cu^{2+} resulted in complex dissociation. Whereas in UV–vis measurements the spectrum was shifted back to the absorption bands of free **3b**, in the EPR spectrum, the signal of the complex was replaced by the signal of free Cu^{2+} (see Supplementary data).

It is well known that fluorescence emission spectroscopy is more sensitive than UV–vis spectroscopy toward small changes, which may affect the electronic properties of molecular receptors. Therefore, fluorescence spectra have also been measured in this study to assess the selectivity of quinoxalone derivatives toward metal ions. Fig. 2(a) shows the fluorescence response of **3b** in ethanol upon addition of different metal cations. It has been observed that the emission spectra (excitation at 418 nm) of free quinoxalone **3b** in ethanol involve two bands, at 474 and 495 nm. Most of these fluorescence bands were quenched when Cu^{2+} ions were added (see a detailed explanation at Section 2.4.2) but could be recovered upon addition of EDTA, meaning the process is reversible. This behavior exhibits a pronounced and selective 'ON–OFF' type of fluorescence response toward Cu^{2+}. However, no distinct responses were observed upon addition of other metal cations (Zn^{2+}, Mg^{2+}, Co^{2+}, Ni^{2+}, Mn^{2+}, Ca^{2+}, Ag^+). By the way, it is noteworthy that **4b** has shown a similar fluorescence quenching behavior (Fig. 2(b)).

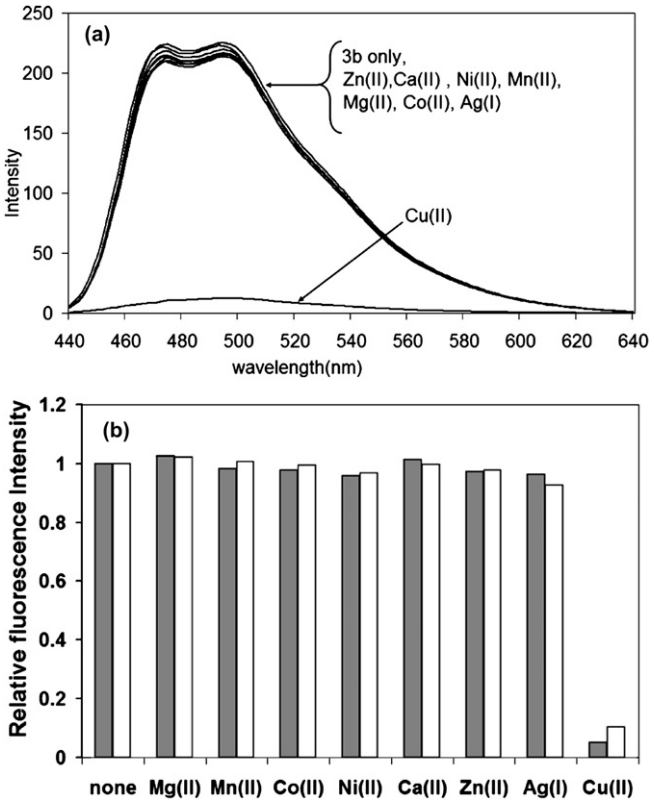

Fig. 2. (a) Fluorescent emission spectra of **3b** (1.2×10^{-5} M) in the absence and presence of Cu^{2+}, Zn^{2+}, Mg^{2+}, Co^{2+}, Ni^{2+}, Mn^{2+}, Ca^{2+}, Ag^{+} (100 equiv) in ethanol (λ_{ex}=418 nm). (b) Relative fluorescence intensities of **3b** (gray) and **4b** (white) (1.2×10^{-5} M) in the presence of 100 equiv of Zn^{2+}, Mg^{2+}, Co^{2+}, Ni^{2+}, Mn^{2+}, Ca^{2+}, Ag^{+} in ethanol (λ_{ex}=418 nm, λ_{em}=475 nm, and λ_{ex}=419 nm, λ_{em}=475 nm respectively).

2.3. The effect of co-existing cations on the response of Cu^{2+} in ethanol

Competition experiments of added Cu^{2+} to **4b** solutions in the presence of one of different metal ions (Zn^{2+}, Mg^{2+}, Ni^{2+}, Mn^{2+}, Ca^{2+}, and Ag^{+}) indicate that the recognition of Cu^{2+} by **4b** was not significantly affected by these co-existing cations, because no change was observed in the red shifted absorption band (except for a slight change in its intensity; see Supplementary data). Therefore, the red shift absorption peak of the complex at 470 nm could be used to monitor Cu^{2+} concentration in ethanol. Similarly, the fluorescence quenching of either **4b** or **3b** in the presence of Cu^{2+} was not significantly affected by the presence of a competing cation.

For comparison, it is noteworthy that quite recently new different fluorescent sensing probes for Cu^{2+} that contain a carbonyl group at the α position of a pyridyl moiety as the metal binding site were reported.[19,20] Mashraqui[20] described an 'ON–OFF' sensor that exhibits a dramatic red shift in the absorption spectra. However, while other cations, such as Li^{+}, Mg^{2+}, Ca^{2+}, and Cd^{2+} did not cause any red shift, the presence of Ni^{2+}, Co^{2+}, and Zn^{2+} did cause a red shift, although much smaller than the one observed with Cu^{2+}.

2.4. Titration experiments and binding stoichiometries

Compounds **3** and **4** differ only in the position of the substituted sulfonamide groups, one at the *meta* and the other at the *para*-position. To further investigate the binding affinity of these compounds to Cu^{2+} and to compare the influence of the position of the sulfonamide moiety on the binding ability in ethanol, Cu^{2+} titration experiments were carried out using compounds **3b** and **4b** as examples.

2.4.1. UV–vis titration experiments. Fig. 3(a) presents the absorption spectra of **3b** in ethanol as a function of added $Cu(ClO_4)_2$. Upon its addition, the absorption intensities of the bands centered at about 393, 418, and 440 nm decrease continuously with concomitant appearance (actually, a red shift occurs) of three new bands at about 419, 441, and 465 nm (due to a red shift) and with increase in their intensities. A similar behavior was also observed by **4b** [Fig. 3(b)].

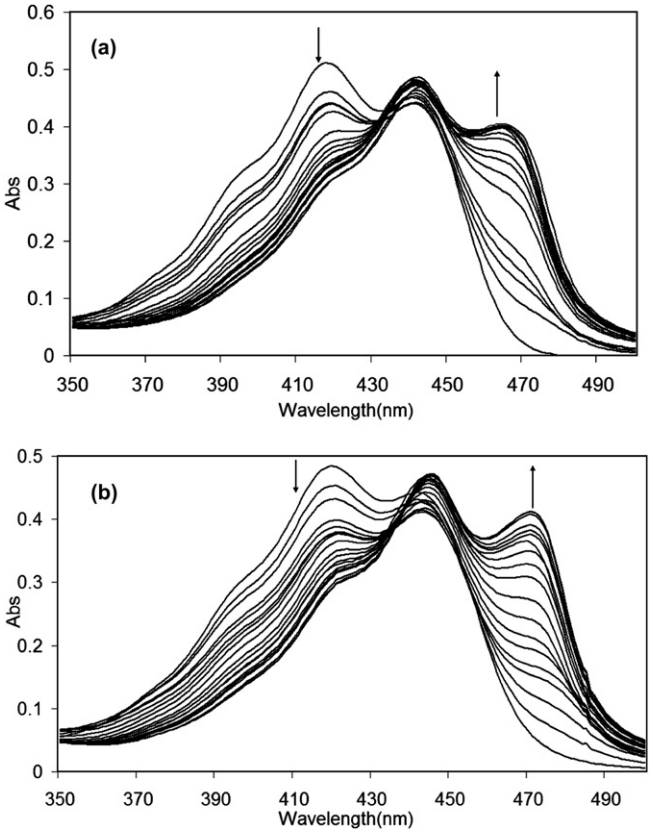

Fig. 3. UV–vis absorption changes of 12 μM of **3b** (a) and **4b** (b) upon addition of increasing amount of Cu^{2+} in ethanol (0, 3, 6, 9, 12, 15, 18, 21, 24, 27, 34.5, 42, 49.5, 57, 64, 72, 79, 87, 117, 147, 177 μM). Arrows indicate the absorbencies that increased (up) and decreased (down) during the titration experiments.

Fig. 4 shows a plot of the absorbance (470 nm) profile of **4b** versus the ratio of $[Cu^{2+}]/[\mathbf{4b}]$. It appears that the binding stoichiometry depends on the total amount of Cu^{2+} added to the organic ligand solution. The plot involves an initial linear increase in absorbance until ~0.5 equiv of Cu^{2+} was added and then, before a plateau was achieved, a second turning point was observed around ~1.1 equiv of Cu^{2+} was added. A similar behavior was also observed by the absorbance (465 nm) profile of **3b**.

Additional examination of the binding stoichiometry in $[Cu^{2+}]/[\mathbf{3b}]$ was done by using MALDI-TOF (as was previously done by others[21]) mass spectrometry, and EPR measurements (see Supplementary data). The MALDI-TOF mass spectrum obtained for **3b** in ethanol in the presence of Cu^{2+} contains signals with *m*/*z* of 515.859, 537.845, 700.940, and 1024.865 that could be assigned to the formation of $[\mathbf{3b}+Cu(II)]^{+}$, $[\mathbf{3b}+Cu(II)-H+Na]^{+}$, $[\mathbf{3b}+Cu(II)+4EtOH+H]^{+}$, and $[2(\mathbf{3b})+Cu(II)+3H_2O]^{+}$ complexes, respectively. The isotopic analysis of these suggested complexes also support these assumptions. Actually, these observations support the existence of 1:1 and 2:1 binding ratio between **3b** and Cu^{2+},

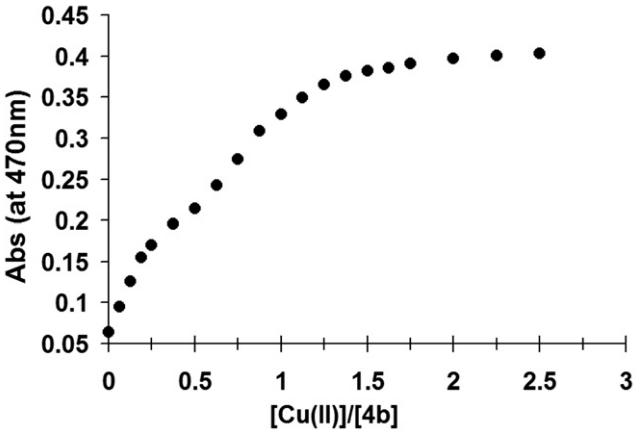

Fig. 4. A plot of absorption of compound **4b** in ethanol versus the ratio [$\mathbf{Cu}^{2+}$]/[**4b**] at 470 nm.

respectively. In addition, EPR titration measurements were carried out by adding increasing amounts of Cu^{2+}. The EPR measurements also support the existence of two different complexes, one predominates at low concentrations of Cu^{2+} (<0.8 equiv) and the other at higher ones. It is important to note that when more than 1 equiv of Cu^{2+} was added to **3b** there was no evidence of a formation of new complex (e.g., with a 1:2 ratio).

Based on the above-mentioned findings, a step-by-step process is suggested (Fig. 5) where first, at low concentrations of Cu^{2+} (<0.5 equiv), a 2:1 complex is formed and later, at higher concentrations of Cu^{2+} (>0.5 equiv) is converted to two possible 1:1 complexes [(A) and (B)] that may contain also ethanol molecules as ligands.

In all the above possible complexes we have assumed that Cu^{2+} binding induced deprotonation of a secondary NH moiety. The structure of compounds **3** and **4** contain two possible binding sites to which Cu^{2+} can bind to form a 1:1 complex with either a six- or four-membered ring [Fig. 5, (a) and (b), respectively]. It is noteworthy that preliminary computations (unpublished, by Zeng's group) of the binding energy of each of the optimized geometries of the suggested complexes (using Gaussian 03) indicate that the 1:1 complex, with a six-membered ring, is the more stable one (by ~17 kcal/mol).

For simplicity, we have estimated (at 418 nm) only the binding constant (*Ks*) for the 1:1 stoichiometry between Cu^{2+} ion and **3b**. The determination of *Ks* was based on the Hildebrand–Benesi equation[3,22] and found to be $(1.15\pm0.07)\times10^5\ M^{-1}$. Similar changes in the absorption spectra were also observed for **4b** upon addition of Cu^{2+}. For a 1:1 stoichiometry of the **4b** complex, *Ks* was estimated as $(3.33\pm0.07)\times10^5\ M^{-1}$.

A non-linear regression analysis (by ReactLab Equilibria program) of the same stoichiometry for **3b** and **4b** afforded binding constants values of $(2.56\pm0.05)\times10^5\ M^{-1}$ and be $(6.93\pm0.01)\times10^5\ M^{-1}$, respectively.

Consequently, it appears that there is an influence of the position of the substituted sulfonamide moiety on the binding constant, as is reflected by its enhancement when the substituent is located at the *para*-position at the 2-oxo-ethylidene side chain compared with the one at the *meta*-position. This is in agreement with the expected electron density donating effect (by resonance) of the sulfonamide substituent being greater at the *para*-position.

It is noteworthy that in a previous work[16] on caffeoyl- or galloyl-containing quinoxalone derivatives linked by an arylamido group, a ratio of 2:1 chelating mode of quinoxalone derivatives to Cu^{2+} was found. This indicates that also the nature of the substituent plays an important role and certainly influences the metal–ligand ratio.

2.4.2. Fluorescence titration experiments. Fluorescence titration experiments were also performed for **3b** and **4b**. Fig. 6 shows that upon exciting at 441 nm, the fluorescence intensity of **3b**, as an example, decreased continuously upon addition of Cu^{2+}, with no significant change in the position of the emission maxima. Since Cu^{2+} is a well-known fluorescence quencher via energy or electron-transfer processes,[23,24] its addition can explain the fluorescence quenching mechanism for types **3** and **4** compounds.

2.5. Evaluation of Cu^{2+} concentrations in ethanol

In order to examine the possibility that the absorbance spectra of either **3b** (at 465 nm) or **4b** (at 470 nm) can be used to quantify the concentration of Cu^{2+}, calibration curves in ethanol were obtained by plotting absorbance as a function of concentration (0.24–1.08 μM) of added Cu^{2+}. Good linear correlations with R^2=0.961 and 0.995, respectively, were obtained. Then samples of either **3b** or **4b** (12 μM) containing 8.95 μM of Cu^{2+} and all other competing cations (8.95 μM of each of Zn^{2+}, Mg^{2+}, Co^{2+}, Ni^{2+}, Mn^{2+}, Ca^{2+}, Ag^{+}) were prepared and absorbencies were measured. The experimental results obtained for both concentrations of Cu^{2+} and absorbencies of its complex with the host are presented in Table 2. They suggest that both complexing agents (**3b** and **4b**) have a potential ability to determine the concentration of Cu^{2+} in

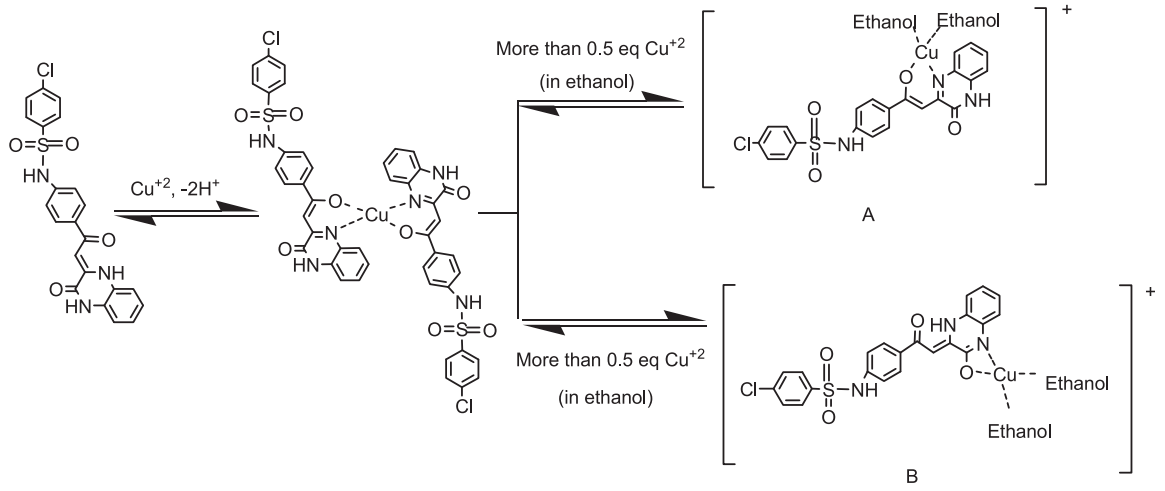

Fig. 5. Proposed stepwise binding processes between Cu^{2+} and **3b**.

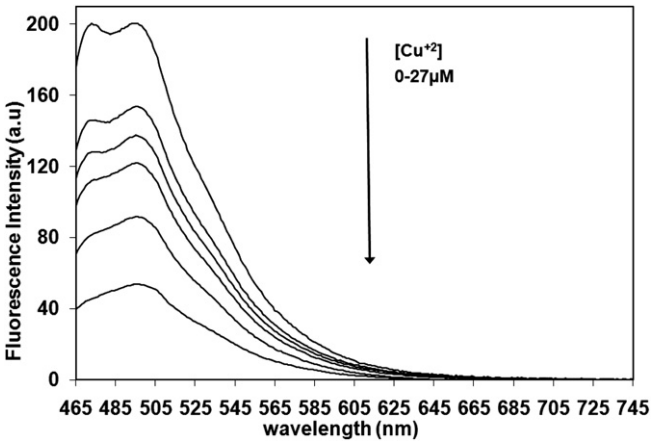

Fig. 6. Fluorescent spectra changes of **3b** (1.2×10^{-5} M) in ethanol upon addition of increasing amounts of Cu^{2+} (from top to bottom: 0, 3, 6, 12, 18, 27 μM); λ_{ex}=441 nm. [Excitation at λ_{ex}=418 nm provided a similar emission spectrum].

ethanol in the presence of various competing cations. It is noteworthy that similar results were obtained either upon addition of a mixture of competing cations to a solution of the host and Cu^{2+} or addition of Cu^{2+} to a pre-prepared mixture of the host and competing cations.

Table 2
Determination of $[Cu^{2+}]$ in EtOH in the presence of competing cations

	$[Cu^{2+}]$ (μM)[a]	$[Cu^{2+}]$ Found[a,b] (μM)	Expected[b] absorbance of complex	Measured absorbance of the complex[a]
3b in EtOH	8.95±0.42	9.30±0.24	0.198±0.020	0.203±0.004
4b in EtOH		8.75±0.52	0.274±0.005	0.270±0.009

[a] In the presence of 8.95 μM of each of the Zn^{2+}, Mg^{2+}, Co^{2+}, Ni^{2+}, Mn^{2+}, Ca^{2+}, Ag^{+} competing cations.
[b] Extracted from calibration curves of absorbance versus $[Cu^{2+}]$ in the presence of **3b** or **4b**.

2.6. UV–vis spectra of 3 and 4 in acetonitrile

The absorption spectra of compounds **3** and **4** in acetonitrile have also been investigated. Similar to the outcome observed in ethanol, there are also two intense bands in the visible region for all compounds studied. For example, **3b** exhibits two bands centered at about 416 and 440 nm with extinction coefficients of 3.3×10^4 and 2.8×10^4 $Lmol^{-1}$ cm^{-1}, respectively (Fig. 7). Compared with ethanol, the wavelengths' maxima in acetonitrile are also quite similar. For example, compounds **3b** and **4b** show λ_{max}=418 and 419 nm, respectively, in ethanol, and 416 and 417 nm, in acetonitrile.

2.7. The effect of metal ions on the UV–vis and fluorescence spectra of 3 and 4 in acetonitrile

2.7.1. UV–vis measurements. Fig. 7(a) describes a typical and representative example of UV–vis spectra for compounds **3** and **4** in acetonitrile, in the presence of different metal ions. Similar to what has already been observed in ethanol, no obvious change was detected in the spectra upon addition of metal cations (Zn^{2+}, Ni^{2+}, Mn^{2+}, Ca^{2+}, Ag^{+}) to the ligand solution. However, when Cu^{2+} was added (Fig. 7(b)), both bands in the visible region disappeared and no distinct new absorption was detected (in the range of 320–800 nm). Also, consistently, the yellowish solutions of **3** or **4**

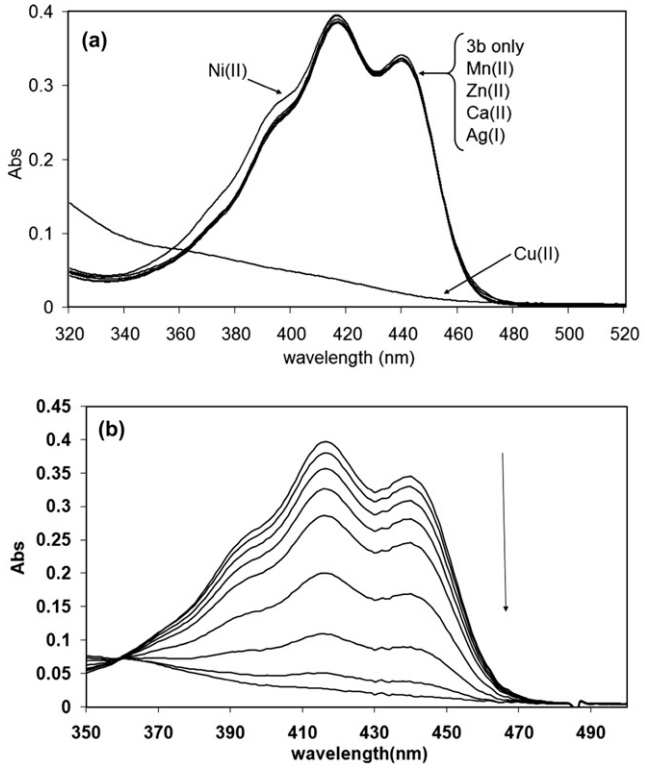

Fig. 7. (a) UV–vis absorption spectra of **3b** in the presence of 100 equiv of metal ions in acetonitrile; [**3b**]=1.2×10^{-5} mol/L; (b) The arrow indicates a decrease in absorbance with increasing amounts of Cu^{2+} (0, 1.5, 3, 4.5, 6, 7.5, 9, 10.5, 12, 13.5,15, 18 μM).

in acetonitrile became colorless. Addition of Cu^{2+} to a solution of **3b** in the presence of other metal ions (Zn^{2+}, Ni^{2+}, Mn^{2+}, Ca^{2+}, Ag^{+}) also caused the disappearance of the light yellow color of **3b**, resulting in a dramatic decrease in the absorbance intensity. It should be pointed out that such a color change has been found to be irreversible because it could not be recovered upon addition of excess of EDTA. In contrast to what was observed in ethanol, this behavior could be attributed to the decomposition of **3b** in the presence of Cu^{2+} in acetonitrile because Cu^{2+} is known to oxidize the nitrogen moiety in similar compounds.[25] The reason for the different behavior in acetonitrile and ethanol stems from the fact that acetonitrile is known to stabilize reduced Cu^{1+}.[26] Since this property causes a color change upon addition of Cu^{2+}, this type of compounds can also be used as 'naked-eye' Cu^{2+} dosimeters in acetonitrile. To support the suggested oxidation-decomposition of **3b** by Cu^{2+} in acetonitrile, EPR measurements were done at room temperature to a sample of **3b** in acetonitrile after adding 2 equiv of Cu^{2+}. The observed EPR signal was that of free Cu^{2+} with no indication of any complex being formed. However, the intensity of the signal was about half of the intensity obtained for 2 equiv of free Cu^{2+}, probably due to partial oxidation of Cu^{2+} to Cu^{1+} (the latter has no EPR signal). Moreover kinetic measurement of the sample showed that the signal for Cu^{2+} gradually diminished and disappeared completely within ~100 min (see Supplementary data).

In order to prove that the organic ligands decompose in acetonitrile, MALDI-TOF measurements of **3b** were conducted upon addition of 2 equiv Cu^{2+}. In comparison with the outcome from ethanol, the results in acetonitrile reveal that a new peak was observed with *m/z* of 905.003. This value suggests a dimer $[(\mathbf{3b})_2-H]$ formation, another evidence for the decomposition of the ligand.

2.7.2. Fluorescence measurements. The fluorescent behavior of compounds **3b** and **4b** was also investigated in acetonitrile. As shown in Fig. 8, **3b** exhibits two intense bands centered at 474 and 495 nm and both totally disappear upon addition of Cu^{2+}. It is plausible that this phenomenon occurs due to the decomposition of the organic ligand by its oxidation with Cu^{2+}. In the case of other cations (after addition of 100 equiv of Zn^{2+}, Ni^{2+}, Mn^{2+}, Ca^{2+} or Ag^{+}), only a slight enhancement of the fluorescence intensity was observed.

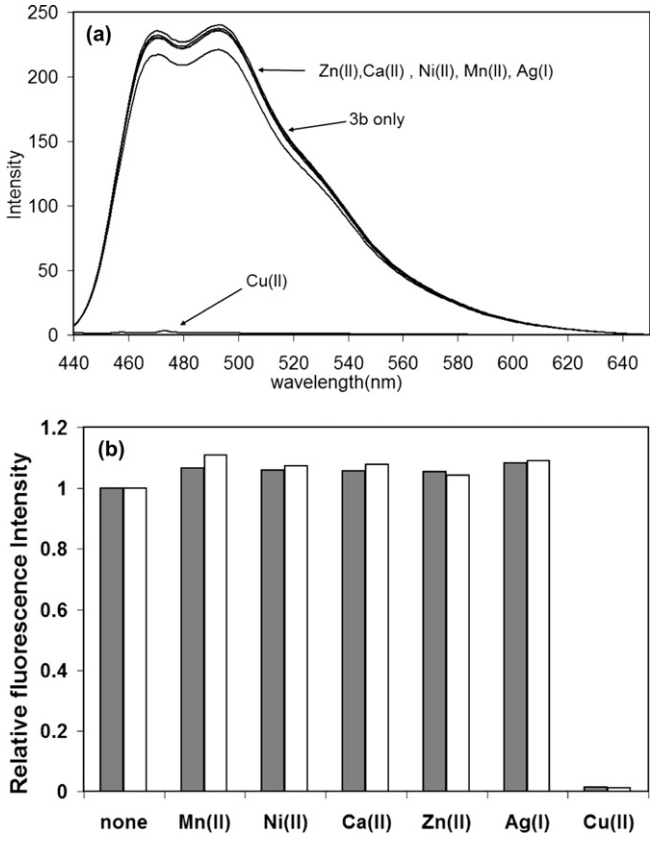

Fig. 8. (a) Fluorescent emission spectra of **3b** (1.2×10^{-5} M) in the absence and presence of Cu^{2+}, Ni^{2+}, Ca^{2+}, Zn^{2+}, Ag^{+}, Mn^{2+} (100 equiv) in acetonitrile; (b) Relative fluorescence intensities of **3b** (gray) and **4b** (white) (1.2×10^{-5} M) in the presence of Cu^{2+}, Ni^{2+}, Ca^{2+}, Zn^{2+}, Ag^{+}, Mn^{2+} (100 equiv) in acetonitrile (λ_{ex}=416 nm, λ_{em}=470 nm for **3b** and λ_{ex}=417 nm, λ_{em}=475 nm for **4b**).

Competition experiments were also carried out by adding Cu^{2+} to **4b** solutions containing an additional metal ion (Zn^{2+}, Ni^{2+}, Mn^{2+}, Ca^{2+} or Ag^{+}). The results indicate that also in acetonitrile, the recognition of Cu^{2+} by **4b** was not significantly affected by either one of the co-existing cations.

3. Conclusions

In conclusion, a series of quinoxalin-2-one derivatives (**3** and **4**) that contain both fluorophore and ionophore integrated into one structural unit has been investigated for their affinity to bind various metal cations. It was found that in ethanol 3b and 4b show a selective red-shift in the UV-vis absorption spectra and a selective fluorescence quenching behavior toward Cu^{2+}, as well as fast and reversible binding. However, no significant response to Zn^{2+}, Mg^{2+}, Co^{2+}, Ni^{2+}, Mn^{2+}, Ca^{2+}, and Ag^{+} was observed. Therefore, they could be utilized as molecular chemosensors for Cu^{2+} in ethanol. In addition, it was found that the position at which the sulfonamide substituent is linked to the central benzene ring affects the binding strength toward Cu^{2+}.

In acetonitrile, **3b** and **4b** behave as dosimeters due to a significant color change originates from oxidation–decomposition of the ligand by Cu^{2+}. Noticeably, this behavior has been found to be exclusive to Cu^{2+} and not to other metal cations.

Finally, these ligands can also be used as a promising building block for the construction of more sophisticated functional chemosensors or chemical switches.

4. Experimental section

4.1. General

The synthesis and characterization of compounds **3** and **4** was described previously.[15]

Absorption spectra were acquired with an Agilent (HP) 8453 UV–vis Diode Array spectrophotometer (single beam) with wavelength accuracy $<\pm0.5$ nm and photometric accuracy $<\pm0.005$ AU.

Fluorescence excitation spectra were acquired with a JASCO spectrofluorometer (Model FP-6500, Jasco Intern. Co., Japan) equipped with a 150 W xenon lamp. Both excitation and emission slit widths were 3 nm. For fluorescence measurements of **3b** and **4b** in ethanol, excitations wavelength at 418 and 419 nm were used, respectively, which were changed to 416 and 417 nm in acetonitrile, respectively. Mass spectra were obtained with MALDI-TOF spectrometer reflex IV (Bruker Daltonic, Germany). EPR spectra were recorded on Bruker EMX-220 X-band ($\nu\sim96$ Hz) EPR Spectrometer.

All measurements were conducted at 25 °C. In the UV–vis measurements the corresponding solvent (ethanol absolute or acetonitrile) was used as blank.

4.2. Reagents and general procedure

The solutions of the metal ions were prepared from Cu^{2+}, Zn^{2+}, Na^{+} as perchlorate salts and Mg^{2+}, Co^{2+}, Ni^{2+}, Mn^{2+}, Ca^{2+}, Ag^{+} as nitrate salts. (Caution: perchlorate salts are potentially explosive). All of the reagents were purchased from commercial suppliers (Aldrich; Merck). For testing the effect of pH 70% $HClO_4$ (Mallinckrodt chemicals) was used and base solution was made from NaOH pellets (Frutarom). The solvents (ethanol or acetonitrile) were obtained from Bio Lab. Israel. Except for solvent that were used in MALDI-TOF measurements all of the chemicals used in this work were of analytical grade and were used without further purification. In MALDI-TOF measurements HPLC graded solvent were used without further purification.

4.2.1. Preparation of sample solutions for the evaluation of selectivity to specific metallic cation. Stock solutions of 1.2×10^{-1} M of Cu^{2+}, Zn^{2+}, Mg^{2+}, Co^{2+}, Ni^{2+}, Mn^{2+}, Ca^{2+}, Ag^{+} were prepared in ethanol and acetonitrile. Stock solutions of hosts (1.2×10^{-5} M) **3b** and **4b** in ethanol and acetonitrile were also prepared. Test samples were prepared by adding 40 μL of each of their mixture metal stock to 4 mL of a host stock solution. For the competition experiment test solutions were prepared by adding 40 μL of the competing cations and 40 μL of Cu^{2+} to 4 mL of the host stock solution.

4.2.2. Preparation of stock solutions and samples for the titration experiments. Stock solutions of 3×10^{-3} M of $Cu(ClO_4)_2$ in ethanol or acetonitrile were prepared. To 4 mL of compound **3b** or **4b** (1.2×10^{-5} M) stock solution was added 0–80 μL of $Cu(ClO_4)_2$ solution.

4.2.3. Evaluation of the effect of added base/acid on the absorption of ligands and complexes. Stock solutions of 2.4×10^{-5} M of **3b**. To Stock solutions of 2.4×10^{-5} M of **3b** in ethanol and of 2.5×10^{-1} M NaOH in tri-distilled water were prepared. To test the effect of base on host in ethanol, 80 μL of NaOH were added to a solution of 4mL

of 3b. To test the acidity effect on copper complex, 80 μL of 70% $HClO_4$ were added to a solution of 4mL of **3b** and 80 μL of Cu^{2+}(1.2×10^{-1} M). (Caution: $HClO^4$ is a strong oxidant and explosive). To test the effect of base on host (**3b**) in ethanol, 80 μL of 70% $HClO_4$ was added to a solution of 4 mL of **3b** (Caution: $HClO_4$ is a strong oxidant).

4.2.4. Preparation of samples for the evaluation the effect competing cations. Calibration curves were obtained by plotting the absorbance (of **3b** at 465 nm and **4b** at 470 nm) as a function of added Cu^{2+}. Test solutions were prepared by adding 3×10^{-3} M of $Cu(ClO_4)_2$ to the host solution. The range of concentrations of added Cu^{2+} was 2.25–16 μM. To test the potential of these hosts to quantify the concentrations of Cu^{2+}, a stock solution of a mixture of 3×10^{-3} M of Zn^{2+}, Mg^{2+}, Co^{2+}, Ni^{2+}, Mn^{2+}, Ca^{2+} and Ag^{+} was prepared in ethanol. Then six repeating samples were prepared for each host by adding 15 μL of the stock solution of the seven competing cations and 15 μL of 3×10^{-3} M of Cu^{2+} to a 5 mL of the host stock solution. The concentration of Cu^{2+} was calculated by using the suitable calibration curve.

4.2.5. Preparation of samples for MALDI-TOF measurements. Stock solutions (1 mM) of **3b** were prepared in either absolute ethanol (dehydrated) or acetonitrile (HPLC graded). Also solutions of $Cu(ClO_4)_2$ in ethanol or acetonitrile (0.1 M) were prepared. For measurements in ethanol three samples were prepared by adding 0.5, 1 or 2 equiv of Cu^{2+} to 2 mL of **3b** in ethanol. For samples in ethanol 2,5-dihydroxybenzoic acid matrix (DHB) (10 mg/mL in 90:10 v/v of deionized water/ethanol) was used. For measurements conducted in acetonitrile the sample was prepared by adding 2 equiv of Cu^{2+} to 2 mL of **3b** in acetonitrile. The matrix for the sample in acetonitrile was prepared by dissolving DHB matrix (20 mg/mL in 2:1 v/v aqua solution of 0.1% trifluoroacetic acid in deionized water/acetonitrile). In both solvents the MALDI samples were prepared by mixing 1 mL of the matrix with 1 mL of the samples containing **3b** in the presence of Cu^{2+}. Then 1 μL of these final samples were loaded onto target plate allowed to dry at room temperature and then analyzed.

4.2.6. EPR measurements. Stock solutions of 4×10^{-2} M $Cu(ClO_4)_2$ were prepared in ethanol and acetonitrile. For the measurements conducted in ethanol titration sample were prepared by adding 15–88 μL of $Cu(ClO_4)_2$ solution to 4 mL of compound **3b** (1 mM). To carry out a qualitative test of the effect of acid on the reversibility of the complex formation, three drops of 70% $HClO_4$ were added to a sample of **3b** containing 40 μL of Cu^{2+} (see Section 2.2 for discussion). Then the signal was re-measured. For the measurements in acetonitrile the sample was prepared by adding 100 μL of $Cu(ClO_4)_2$ solution to 2 mL of compound **3b** (1 mM) and then the signal was re-measured several times after that during the next 180 min. Also the signal of free 2 mM Cu^{2+} in acetonitrile was measured.

Acknowledgements

This work was supported by grants from the National Basic Research Program of China (No. 2009CB930200), Beijing Novel Project (No. 7112008), and Beijing City Education Committee (KM201010005009). The authors gratefully acknowledge Dr. A.I. Shames for performing and analyzing all EPR spectra in this work. E.K., B.C., and J.Y.B. are thankful to Mrs. E. Solomon for technical assistance.

Supplementary data

Supplementary data associated with this article can be found in the online version, at doi:10.1016/j.tet.2011.06.047. These data include MOL files and InChiKeys of the most important compounds described in this article.

References and notes

1. de Silva, A. P.; Gunaratne, H. Q. N.; Gunnlaugsson, T.; Huxley, A. J. M.; McCoy, C. P.; Rademacher, J. T.; Rice, T. E. *Chem. Rev.* **1997**, *97*, 1515–1566.
2. Amendola, V.; Fabbrizzi, L.; Foti, F.; Licchelli, M.; Mangano, C.; Pallavicini, P.; Poggi, A.; Sacchi, D.; Taglietti, A. *Coord. Chem. Rev.* **2006**, *250*, 273–299.
3. Valeur, B. *Molecular Fluorescence, Principles and Applications*; Wiley-VCH: Weinheim, 2001.
4. Singhal, N. K.; Ramanujam, B.; Mariappanadar, V.; Rao, C. P. *Org. Lett.* **2006**, *8*, 3525–3528.
5. Qi, X.; Jun, E. J.; Xu, L.; Kim, S.-J.; Joong Hong, J. S.; Yoon, Y. J.; Yoon, J. *J. Org. Chem.* **2006**, *71*, 2881–2884.
6. Xu, Z.; Xiao, Y.; Qian, X.; Cui, J.; Cui, D. *Org. Lett.* **2005**, *7*, 889–892.
7. Park, S. M.; Kim, M. H.; Choe, J.-I.; No, K. T.; Chang, S.-K. *J. Org. Chem.* **2007**, *72*, 3550–3553.
8. Xiang, Y.; Tong, A.; Jin, P.; Ju, Y. *Org. Lett.* **2006**, *8*, 2863–2866.
9. Zhang, X.; Shiraishi, Y.; Hirai, T. *Org. Lett.* **2007**, *9*, 5039–5042.
10. Gunnlaugsson, T.; Leonard, J. P.; Murray, N. S. *Org. Lett.* **2004**, *6*, 1557–1560.
11. Martinez, R.; Zapata, F.; Caballero, A.; Espinosa, A.; Tarraga, A.; Molina, P. *Org. Lett.* **2006**, *8*, 3235–3238.
12. Hazuda, D. J.; Felock, P. *Science* **2000**, *287*, 646–650.
13. Hazuda, D. J.; Young, S. D.; Cuare, J. P.; Anthony, N. J.; Gomez, R. P.; Wai, J. S.; Vacca, J. P.; Handt, L.; Motzel, S. L.; Klein, H. J.; Dornadula, G.; Danovich, R. M.; Witmer, M. V.; Wilson, K. A.; Tussey, L.; Schleif, W. A.; Gabryelski, L. S.; Jin, L.; Miller, M. D.; Casimiro, D. R. *Science* **2004**, *305*, 528–532.
14. Zhuang, L.; Wai, J. S.; Embrey, M. W.; Fisher, T. E.; Egbertson, M. S.; Payne, L. S.; Guare, J. P.; Vacca, J. P.; Hazuda, D. J.; Felock, P. J.; Wolfe, A. L.; Stillmock, K. A.; Witmer, M. V.; Moyer, G.; Schleif, W. A.; Gabryelski, L. J.; Leonard, Y. M.; Lynch, J. J.; Michelson, S. R.; Young, S. D. *J. Med. Chem.* **2003**, *46*, 453–456.
15. Zeng, C.-C.; Li, X.-M.; Yan, H.; Zhong, R.-G. *Chin. J. Chem.* **2007**, *25*, 1174–1182.
16. Xu, Y. S.; Zeng, C.-C.; Li, X. M.; Zhong, R.-G.; Zeng, Y. *Chin. J. Chem.* **2006**, *24*, 1086–1094.
17. Li, X.-M.; Zeng, C.-C.; Niu, L.-T.; Yan, H.; Zheng, D. W.; Zhong, R.-G. *Chem. Res. Chin. Univ.* **2006**, *22*, 747–752.
18. Li, X.-M.; Zeng, C.-C.; Xu, Y.-S.; Yan, H.; Zheng, D. W.; Zhong, R.-G. *J. Chem. Crystallogr.* **2006**, *36*, 357–363.
19. Lin, W.-Y.; Yuan, L.; Cai, X.-W.; Tan, W.; Feng, Y.-M. *Eur. J. Org. Chem.* **2008**, *29*, 4981–4987.
20. Mashraqui, S. H.; Khan, T.; Sundaram, S.; Ghadigaonkar, S. *Tetrahedron Lett.* **2008**, *49*, 3739–3743.
21. Singhal, N. K.; Mitra, A.; Rajsekhar, G.; Shaikh, M. M.; Kumar, S.; Guionneau, P.; Rao, C. P. *Dalton Trans.* **2009**, *39*, 8432–8442.
22. Connors, K. A. *Binding Constants—The Measurement of Molecular Complex Stability*; John Wiley: New York, NY, 1987.
23. Varnes, A. W.; Dodson, R. B.; Wehry, E. L. *J. Am. Chem. Soc.* **1972**, *94*, 946–950.
24. Kemlo, J. A.; Shepherd, T. M. *Chem. Phys. Lett.* **1977**, *47*, 158–162.
25. Sumalekshmy, S.; Gopidas, K. R. *Chem. Phys. Lett.* **2005**, *413*, 294–299.
26. Kurnia, K.; Giles, D. E.; May, P. M.; Singh, P.; Hefter, G. T. *Talanta* **1996**, *43*, 2045–2051 and references therein.